Geomorphology 290 (2017) 365–375

Contents lists available at ScienceDirect

Geomorphology

journal homepage: www.elsevier.com/locate/geomorph

Variations in spatial patterns of soil-vegetation properties and the emergence of multiple resilience thresholds within different debris flow fan positions

Neda Mohseni[a], Seyed Reza Hosseinzadeh[a,*], Adel Sepehr[b], Mahmood Reza Golzarian[c], Farzin Shabani[d]

[a] Department of Geography, Ferdowsi University of Mashhad, Mashhad, Iran
[b] Department of Desert and Arid Zone Management, Ferdowsi University of Mashhad, Mashhad, Iran
[c] Department of Biosystems Engineering, Ferdowsi University of Mashhad, Mashhad, Iran
[d] Ecosystem Management, School of Environmental and Rural Science, University of New England, Armidale 2351, Australia

ARTICLE INFO

Keywords:
Debris flow fan
Vegetation
Soil characteristics
Resilience thresholds

ABSTRACT

Debris flow fans are non-equilibrium landforms resulting from the spatial variations of debris flows deposited on them. This geomorphic disturbance involving the asymmetric redistribution of water and sediment may create spatially heterogeneous patterns of soil-vegetation along landforms. In this research, founded on field-based observations, we characterized the spatial patterns of some soil (*e.g.*, particle size distribution including fine and coarse covers, and infiltration capacity) and vegetation (*e.g.*, plant distance, vegetation density, patch size, and average number of patches) properties within different debris flow fan positions (Upper, Middle, and Lower fan) located at the base of the Binaloud Mountain hillslope in northeastern Iran. Thereafter, using a mathematical model of dry land vegetation dynamics, we calculated response trends of the different positions to the same environmental harshness gradient. Field measurements of soil-vegetation properties and infiltration rates showed that the asymmetric redistribution of debris flow depositions can cause statistically significant differences ($P < 0.05$) in the spatial patterns of soil and eco-hydrological characteristics along different landform positions. The results showed that mean plant distance, mean vegetation density, and the average number of patches decreased as the coarse covers increased toward the Lower fan plots. Conversely, an increase in infiltration rate was observed. The simulation results on the aerial images taken from different positions, illustrated that positions with a heterogeneous distribution of vegetation patterns were not desertified to the same degree of aridity. Thus, the Middle and Lower positions could survive under harsher aridity conditions, due to the emergence of more varied spatial vegetation patterns than at the Upper fan position. The findings, based on a combined field and modeling approach, highlighted that debris flow as a geomorphic process with the asymmetric distribution of depositions on the gentle slope of an alluvial fan, can incur multiple resilience thresholds with different degrees of self-organization under stressful conditions over the spatial heterogeneities of soil-dependent vegetation structures.

1. Introduction

One of the critical characteristics of arid regions is the heterogeneous distribution of vegetation structures as vegetated mosaics bordered by barren interspaces. Degradation of vegetation patches and expansion of bare soils result in the formation of irregular and regular vegetation patterns such as bands (Saco et al., 2007; McDonald et al., 2009; Merino-Martín et al., 2012), labyrinths (Rietkerk et al., 2004), spots (Couteron and Lejeune, 2001), and rings (Ravi et al., 2008; Cartenì et al., 2012; Meron, 2012) over time. These patterns are a signal of decreasing landscape resilience to degradation (Scheffer et al., 2001; Rietkerk et al., 2002; Kéfi et al., 2007; Scheffer et al., 2009; Dakos et al., 2011; Moreno-de las Heras et al., 2011). Many researchers have claimed that resource concentration mechanisms are effective in the expansion of fragmented landscapes (van de Koppel et al., 2002; van de Koppel and Rietkerk, 2004; D'Odorico et al., 2007; Kéfi et al., 2010; Ravi et al., 2010; Turnbull et al., 2012). These mechanisms founded on the asymmetric redistribution of water, nutrients and sediment can

* Corresponding author at: Department of Geography, Ferdowsi University of Mashhad, Azadi Square, Mashhad 9177-948-978, Iran.
E-mail addresses: neda.mohseni@mail.um.ac.ir (N. Mohseni), srhosseinzadeh@um.ac.ir (S.R. Hosseinzadeh).

http://dx.doi.org/10.1016/j.geomorph.2017.04.023
Received 27 October 2016; Received in revised form 4 February 2017; Accepted 13 April 2017
Available online 17 April 2017
0169-555X/

create the spatial heterogeneities in the patterns of soil and vegetation properties (Ludwig et al., 2005; Breshears et al., 2009). The emergence of such heterogeneous patterns results in increasing interactions between biotic and abiotic structures within the landscape, such as vegetation and soil (Turnbull et al., 2010). These interactions cause that fragmented landscapes simultaneously exhibit a contradictory desirable and hostile environment. This means that, in the vegetated mosaics, a higher density of plants lead to an increase in water infiltration and nutrient availability, decreased evaporation from the top soil and, subsequently more stability of plant in the face of perturbations. Conversely, such desirable situations do not happen for sparsely vegetated and barren soils. These contradictory conditions can exhibit multiple resilience thresholds with varying degrees of sustainability across the landscape, in reaction to external forces. Many abiotic processes such as geomorphic disturbances (*e.g.*, hydro-aeolian erosion and, different types of landslides) can contribute to the emergence and expansion of such conditions. These processes promoting heterogeneity in the spatial distribution of resources, encourage the occurrence of asymmetric patterns in soil and vegetation properties.

Debris fans may be described as non-equilibrium landforms resulting from the spatial variability of sediments involved in different types of landslides including debris flows, flash floods, sheet floods, other hyperconcentrated flows. In many arid and semi-arid regions, landslides constitute one of the dominant geomorphic disturbances with the potential to modify the landscape (Walker and Shiels, 2012). Landslide is a generic term for a variety of movements of masses comprising materials such as earth, debris, rock, organics materials, such as debris flows, rock falls, earth slides and, mudflows (Cruden and Varnes, 1996; Geertsema and Pojar, 2007; Geertsema et al., 2009). Thus, by definition, debris flows constitute a variety of landslide that transports a mass of rock fragments, mud, soil, and water down a slope (Cruden and Varnes, 1996), and through a channel or gully depositing the debris on a fan (Geertsema and Highland, 2011). Debris refers to loose and unsorted materials, consisting of a mix of gravel, pebbles, cobbles and boulders in a matrix of sand, silt, and clay (Hungr et al., 2001; Geertsema et al., 2010). Debris flows transporting runoff and sediment along a gentle surface of an alluvial fan are a critical agent in the emergence of spatial biotic-abiotic heterogeneities at the landscape level (Dorin Alexandru and CHIŢU, 2013). The process of introducing different materials into, or removing materials from, a given site can trigger heterogeneity in soil biotic (plants and soil organisms) and abiotic (soil physiochemical) properties (Geertsema et al., 2010; Walker and Shiels, 2012), which can lead to the development of novel local habitats for colonizing organisms (Walker and Shiels, 2012). Landslides (including debris flows) have a significant impact on site, soil, and vegetation diversity (Geertsema and Pojar, 2007). One of the factors that may lead to such diversity is the spread of flow on the fan level, due to the increased in width of the fan (Bull, 1963). Spatial variability in the distribution of flow-induced sediments can encourage heterogeneous spatial patterns in soil and vegetation properties, and subsequently create site conditions which may exhibit multiple resilience thresholds within different landform positions along the slope of debris fan.

The role played by many geomorphic processes and variables in the occurrence of biotic-abiotic heterogeneities have been studied in part. Ravi et al. (2007, 2008, 2009) and Breshears et al. (2009) investigated the role of hydro-aeolian processes in the variations of patterns of soil and vegetation in arid landscapes. Geertsema and Pojar (2007), and Geertsema et al. (2009) have shown how landslides, as geomorphic disturbances changing site, soil, and vegetation can provide biodiversity at the landscape level. Marston (2010) focused on the interactions between vegetation and hillslope geomorphology and their impact on landscape evolutionary trends. Dorin Alexandru and CHIŢU (2013) studied the influence of habitat structures created by landslides on pond-dependent fauna species, and its potential in biodiversity conservation. However, there is limited research on how debris flows as geomorphic disturbance causing biotic-abiotic heterogeneities at landscape level, can affect landscape resilience in the face of environmental stresses.

In this study, we characterize some of causes and consequences of landscape heterogeneity. Incorporating a combined field and modeling approach we established the following objectives:

1. To investigate the cause of landscape heterogeneity: using a simple conceptual approach based on data obtained from field observations, we investigated how debris flows with the asymmetric distribution of depositions along a gentle slope of a debris fan, can exhibit fine scale heterogeneities in the spatial patterns of soil and vegetation properties within different landform positions.
2. To predict the consequence of landscape heterogeneity: using a mathematical modeling approach we demonstrated how biotic-abiotic heterogeneities resulting from variation of debris flow depositions can exhibit multiple resilience thresholds with different self-organization degrees within different debris fan positions under the same rainfall gradient.

2. Materials and methods

2.1. Study area

This research was implemented on a debris flow fan located at the base of Binaloud Mountain hillslope in Neyshabur county, Khorasan-e Razavi province in northeastern Iran approximately within latitude 36°10′N and longitude 58°59′E (Fig. 1).

According to the De Martonne classification method, the study area's climate is semi-arid with mean annual temperature of 12.9 °C and approximately 235 mm mean annual precipitation. The catchment of the study fan is located on the southern Binaloud Mountain at an elevation approximately 3080 m. The drainage pattern of the catchment comprises dendritic and parallel patterns. The almost 4 km, main stream of the catchment plays an important role in sediment transport on the fan, and the catchment of the fan is composed mainly of fillet, schist, conglomerate and lime stone. The climatic, geomorphic (high elevation and steep slope), and geological (lithological) characteristics encourage extreme mechanical weathering and subsequent high erosion rates in the catchment, which promote landslide, in the event of intense rainfall. During heavy rainfall, sediment-laden water from the fan catchment is concentrated into channels flowing down the slope, eventually crossing the fan surface. Debris flow depositions consist of a various distribution of sizes from clay to boulders. Due to the characteristics of the catchment lithology, sediments deposited on the fan are composed mainly of clay, silt, and gravel. Further, after intense floods, which mostly occur in late winter and early spring, the fan transports a clast-supported pebble-to-boulders diversity of materials. These geomorphic events can result in a broad heterogeneity in soil biotic-abiotic properties within different landform positions.

2.2. Field methods

To characterize variability in the spatial patterns of soil and vegetation properties within different debris fan positions, this landform was classified to three positions perpendicular to the slope: the Upper, Middle, and Lower fan with 15 m elevation distances at approximately 1380 m, 1365 m, and 1350 m, respectively (Fig. 2). At each position we randomly established three replicate 10 by 10 m plots (sub-position plots) for measuring soil properties and vegetation metrics.

To conduct the experiments and soil sampling, each plot was divided into twenty-five 2 by 2 m blocks. The aim of dividing the plots was that the points of experiments and soil sampling could be co-located. All experiments and soil sampling were done at the center of the blocks. Experiments for determining the infiltration capacity of

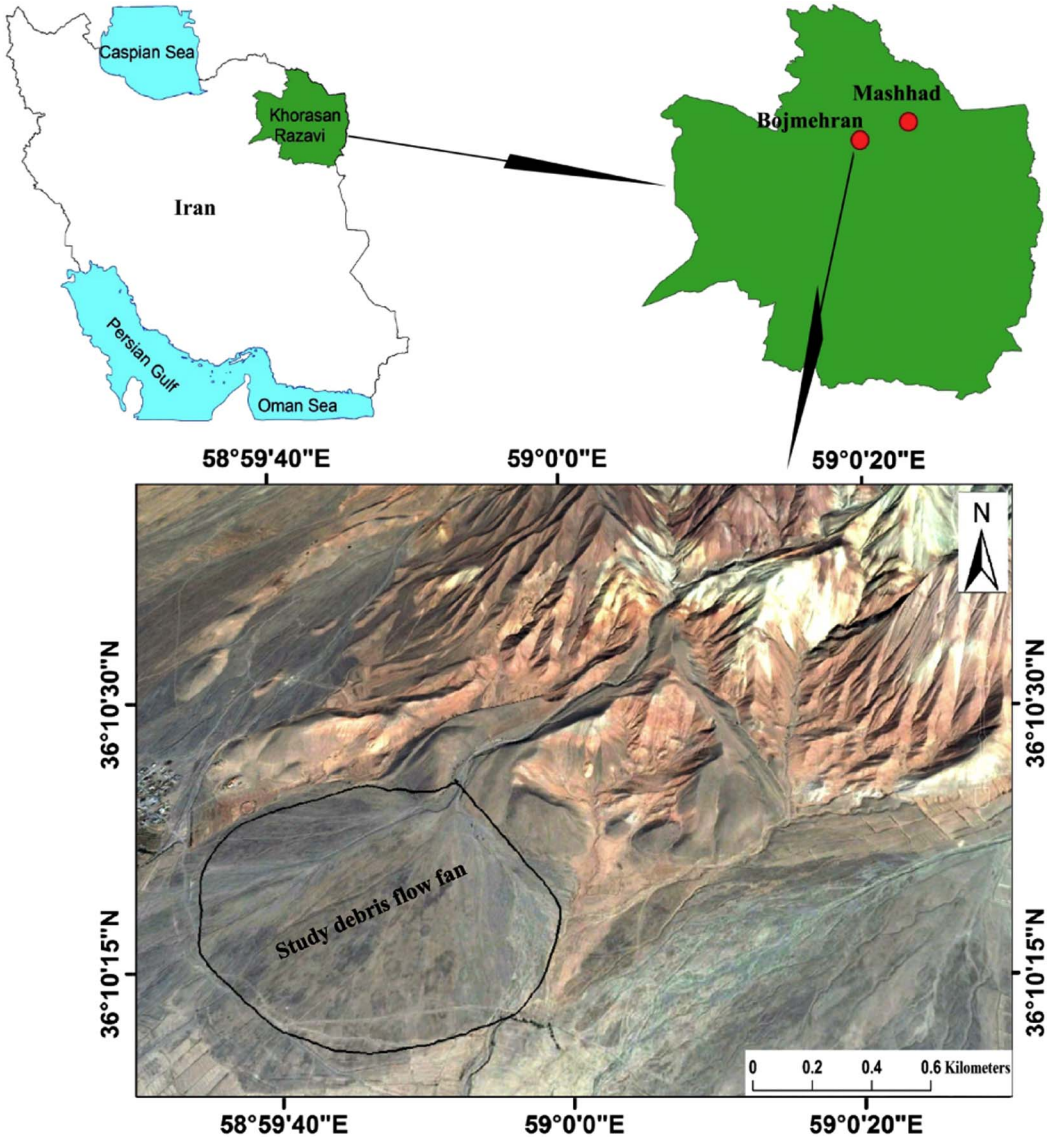

Fig. 1. Location of the study area, which is a debris flow fan.

water to soil under unsaturated conditions (K) were conducted using a mini-disk infiltrometer (Decagon Devices, Inc., USA). This method of measuring infiltration rate was ideal at the study site because of the small size of sampling blocks within each plot.

For analyzing particle size distribution, which is an effective factor of soil infiltration rate, soil water, and nutrient content holding capacity (Graetz and Tongway, 1986; Wood et al., 1987; Turnbull et al., 2010), soil samples were co-located with hydraulic conductivity measurement. Since sediment entrainment and transport processes affect surface soil layer (Wainwright et al., 2000; Turnbull et al., 2010), soil samples were collected from a 0–5 cm depth, *i.e.* the uppermost soil layer. The collected soil samples were air-dried and passed through a 2 mm sieve for determining the distribution of soil fractions ≤ 2 mm (the percentage of clay, silt, and sand) using the standard hydrometer method (ASTM 152H) (Bouyoucos, 1962). The percentage of the fractions ranging between 2 and 12 mm in diameter (fine pebble) was determined using a mechanical sieve shaker (Sieve Analysis), which quantifies the percentage of aggregates by passing dry soil samples passed through 2, 4, 12 mm meshes. Finally, the data from infiltration experiments and soil samples analyses within three sub-position plots were pooled together (overall, 75 observations in each position).

To determine spatial patterns of vegetation properties within different debris fan positions, a set of vegetation metrics were characterized by taking high-resolution (1 m) aerial images from a height of 10 m above each plot (Fig. 2). Aerial images were taken by a quadcopter drone equipped with GoPro HERO4 12-megapixel digital camera. The aerial images were read and processed in MATLAB (ver. R2013a; Mathworks Inc., US) for information extraction purposes. To eliminate the possibility of software errors in the differentiation of vegetated and barren mosaics, due to low color contrast between both the mosaics, we separated manually the boundary between vegetated and barren patches in each image. Thereafter, the aerial images were converted to binary images using a thresholding method. The resulting segmented binary images were images of the same size as the original image and if the pixels belong to vegetated patches they were white, otherwise black (Fig. 3). In the next processing step, which was the feature extraction step, all binary images were partitioned into twenty-five 2 by 2 m blocks. From each block and also all blocks of each image, mean plant distance - the distance of each shrub to its nearest neighbor, mean plant density, mean patch size and average number of patches were calculated. Finally, data from all three sub-position plots were integrated.

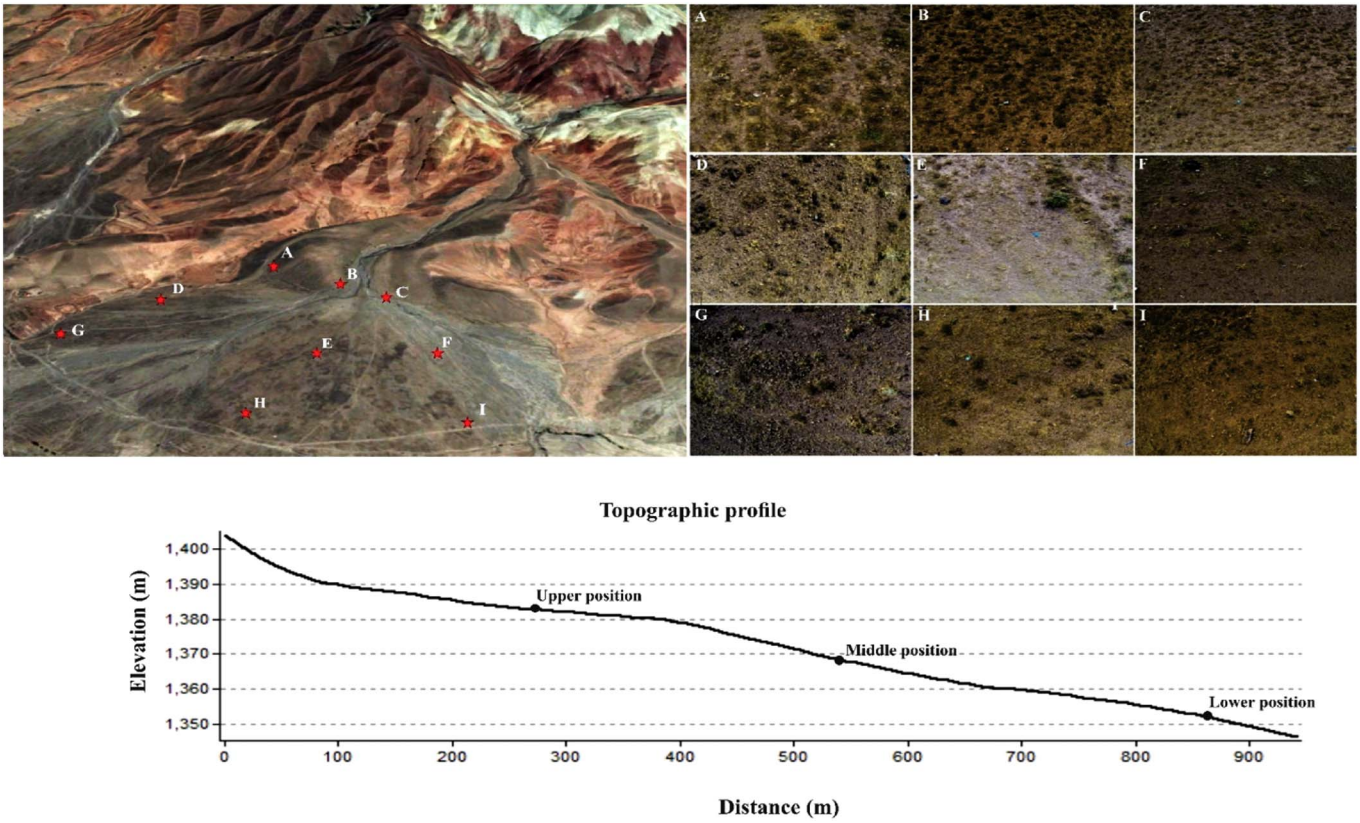

Fig. 2. Top left-hand panel: positions of sampling plots (red stars) within the study debris fan defined by GPS. Top right-hand panel: Aerial images taken from above each sampling plot: Images (A, B, C), (D, E, F), and (G, H, I) are images of plots associated with the Upper, the Middle, and the Lower fan positions, respectively. Bottom panel: topographic profile showing the approximate elevation of each position. (For interpretation of the references to color in this figure legend, the reader is referred to the web version of this article.)

2.2.1. Statistical analyses

A one-way ANOVA analysis (analysis of variance) followed by a Tukey *post hoc* test was conducted to compare the differences of soil properties (infiltration rate and particle size distribution) and the vegetation properties (plant distance, plant density, patch size and, the average number of patches) among the Upper, the Middle, and the Lower debris fan positions. The Kolmogorov–Smirnov test was employed for verifying the normality and the distributional adequacy of the datasets. The results of this test showed that the soil samples data were relatively normally distributed. Further, the vegetation data had a normal distribution, following a log-10 transformation. All statistical analyses were performed using the software program SPSS (ver. 16.0, IBM, US). The probability level (P value) for all statistical analyses was set at 0.05.

2.3. The model description

For comparison of the behavior of different debris fan positions in the face of similar environmental stresses, a mathematical model originally developed Rietkerk et al. (2002) and later modified by Kéfi et al. (2010) was run on the corresponding binary forms of some aerial images taken from three different positions of the Upper, Middle and Lower fans at the studied area (Fig. 3). This model describes spatial vegetation dynamics in arid ecosystems (Kéfi et al., 2010): One of the critical characteristics of arid landscapes is the heterogeneous distribution of vegetation structures as vegetated and barren mosaics (d'Herbès et al., 2001). This characteristic causes an infiltration contrast between vegetated (higher infiltration) and barren (lower infiltration) mosaics (Tongway and Ludwig, 2001). When rainfall occurs, the ground with a high plant density gathers a greater quantity of water (sink area), while runoff is generated on barren soils (source area) due to their low infiltration capacity (Kéfi et al., 2010). This condition, in terms of the activation of resource concentration mechanisms, results in the emergence of the interactions between water infiltration, soil, and plant: higher resources accumulation on the vegetated area due to higher capacity for water infiltration and uptake, than on barren soils. All these conditions are assumed in the above-mentioned model. Note that, in this model the main mechanism driving the vegetation patterns dynamic is the difference in infiltration rate between vegetated and barren areas, represented as the Wo in the formulation of the model (Kéfi et al., 2010).

The model formulation consists of three partial differential equations that describe the dynamics of three variables: vegetation biomass (P) in $g\,m^{-2}$, soil water (W) in mm, and surface water (O) in mm (HilleRisLambers et al., 2001; Rietkerk et al., 2002; Kéfi et al., 2010). It is a noteworthy point that the interaction between these variables forms a critical mechanism in spatial vegetation dynamics and, subsequently arid landscapes evolution. The vegetation biomass (P) in Eq. (1), soil water uptake (W) in Eq. (2), and surface water (O) in Eq. (3) is time dependent, denoted by (t) and updated according to these PDEs:

$$\frac{\partial P(t)}{\partial t} = C \times g_{max} \times \frac{W}{W + K_1} \times P - d \times P + D_P \Delta P \tag{1}$$

$$\frac{\partial W(t)}{\partial t} = \propto O \frac{P + K_2 W_0}{P + K_2} - g_{max} \times \frac{W}{W + K_1} \times P - r_w W + D_w \Delta W \tag{2}$$

$$\frac{\partial O(t)}{\partial t} = \mathrm{R} - \frac{\propto O (P + k_2 W_0)}{P + K_2} - I_0 O + D_0 \Delta O \tag{3}$$

where C is the conversion of water uptake by plants to plant growth (in grams per millimeter per square meter), d is the specific loss of plant density due to mortality (per day), and D_P is the plant dispersal (in square meters per day) g_{max} is the maximum specific water uptake (in millimeters per gram per square meter per day), K_1 is the half-saturation constant of specific growth and water uptake (in milli-

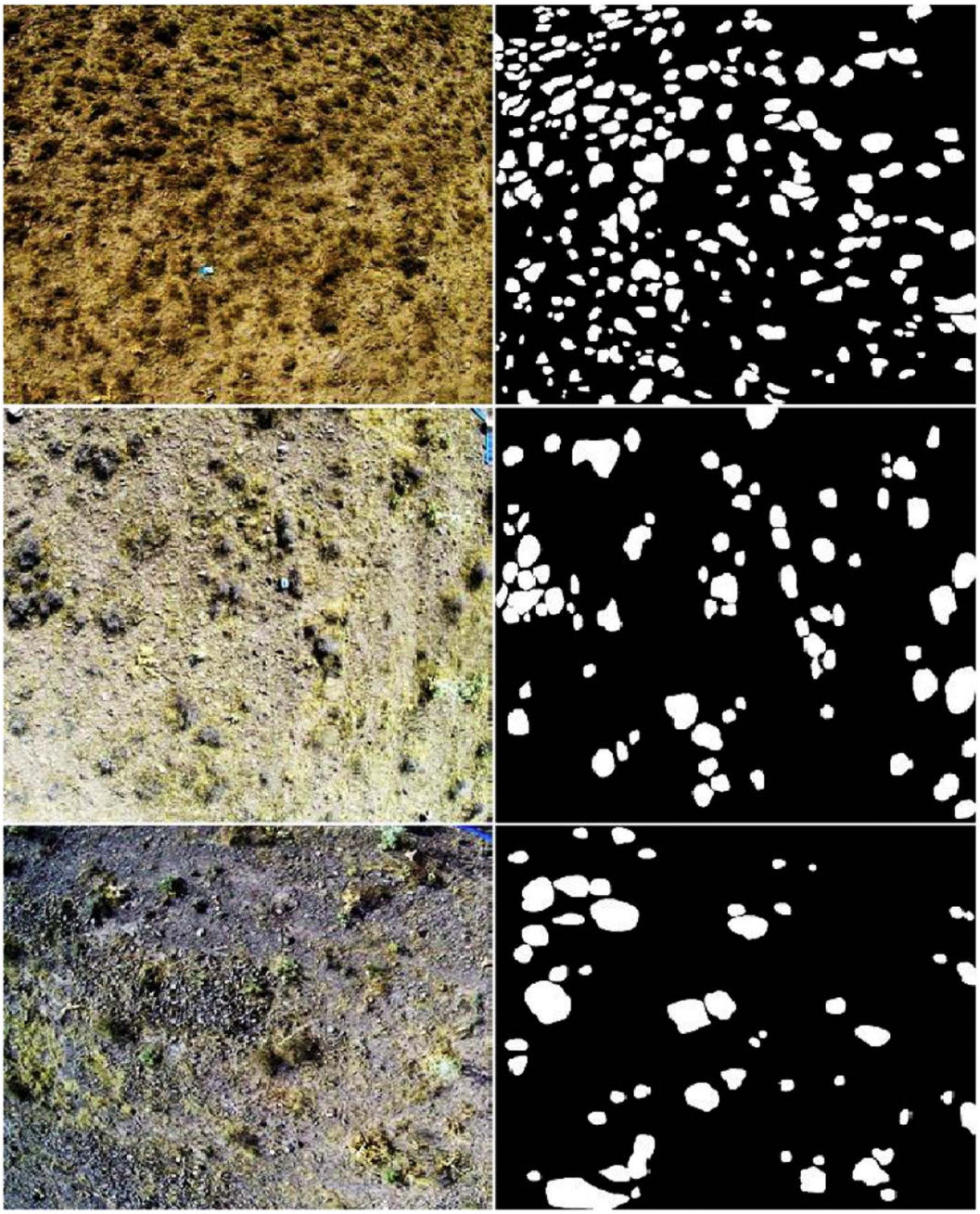

Fig. 3. Representative color aerial images taken from different landform positions and their corresponding binary images that were used as the inputs to the simulation model. The images from top to bottom correspond to the Upper, Middle, and Lower fan positions, respectively. In binary images, white and black areas pixels are associated with vegetated mosaics and barren grounds, respectively. (For interpretation of the references to color in this figure legend, the reader is referred to the web version of this article.)

meters), r_w the soil water loss due to evaporation and drainage (per day), D_w is the diffusion coefficient for soil water (in square meters per day), R is the rainfall (in millimeters per day), $\propto$ is the maximum infiltration rate (per day), K_2 is the saturation constant of water infiltration (in grams per square meter), W_0 is a rate of the infiltration contrast between vegetated and bare soils (dimensionless), D_0 is the diffusion coefficient for surface water (in square meters per day), Δ is the Laplace operator in x and y, and I_0 is the surface water loss rate due to formation of runoff (per day). For all parameters, we used the initial values explained in Kéfi et al. (2010), and as follows:

$C = 10(\mathrm{g\,mm^{-1}m^{-2}})$, $d = 0.25\ (\mathrm{d^{-1}})$, $D_P = 0.1(\mathrm{m^2d^{-1}})$, $g_{max} = 0.05(\mathrm{mm\,g^{-1}m^2d^{-1}})$,

$K_1 = 5(\mathrm{mm})$, $r_w = 0.2(\mathrm{d^{-1}})$, $D_w = 0.1(\mathrm{m^2d^{-1}})$, $\propto$=$0.2(\mathrm{d^{-1}})$, $K_2 = 5(\mathrm{g{\cdot}m^{-2}})$, $W_0 = 0.2$ (—),

$\mathrm{D_0} = 100(\mathrm{m^2d^{-1}})$, $I_0 = 0(\mathrm{d^{-1}})$

2.3.1. Image processing: numerical simulations and analyses

Numerical simulations based on the above described model were repeated for each of the aerial images. Images of Upper, Middle, and Lower positions of the fan formed the inputs to the model. All initial values for the parameters in the model were maintained for each input image. It should be noted that the initial condition, in terms of the spatial distribution of vegetation structures for running the model,

differed from earlier studies (Rietkerk et al., 2002; Kéfi et al., 2010; Dakos et al., 2011) based on current conditions in the study area. As aridity is a determining factor in the occurrence of desertification in arid ecosystems (Dakos et al., 2011), the level of aridity was considered as environmental harshness and was determined by changing rainfall values (parameter R). Simulations started from a current state of each position, with changing rainfall values graded in small steps over 1000 time steps (years). For each level of rainfall value, simulations were run until each position reached a stationary state. This process was repeated until the rainfall reached a critical threshold at which the position's state collapsed toward uniform barren state (desert). For calculating the response trends of each position to changes of rainfall values, we used equilibrium values of total vegetation density for each rainfall value up to the collapse of vegetation. Simulations and running the model in the study area aerial images were performed in Matlab (ver. R2013a; Mathworks Inc., US).

3. Results

3.1. Variations in spatial patterns of soil-vegetation properties within debris fan

The results of the statistical analyses showed that there were significant differences ($P < 0.05$) in hydraulic conductivity rate and particle size distribution ≤ 2 mm (fine cover) separated from clay fraction, especially 2–12 mm fractions (coarse cover), between the Upper, Middle, and Lower fan (Table 1).

The results of statistical analysis from the infiltration experiments indicated that mean hydraulic conductivity (K) value was higher at the Lower fan compared with the Upper position (Table 1; Fig. 4a). The Middle position also had an intermediate infiltration rate between the Upper and Lower positions (Table 1; Fig. 4a). In term of particle size distribution, the highest and the lowest percentages of silt were seen on the Upper and Middle fan, respectively. The Lower fan was intermediate in this regard (Table 1; Fig. 4b). The Upper fan exhibited the highest amount of sand fraction, while the Middle and Lower positions showed the lowest amount of sand (Table 1; Fig. 4b). The maximum percentage of coarse cover (fine pebbles) was found on the Middle and Lower positions, while the Upper fan exhibited the minimum amount of these soil particles (Table 1; Fig. 4b).

The results of the statistical analyses showed that the vegetation metrics varied significantly within different debris fan positions ($P < 0.05$) (Table 2). Overall, according to the results of one-way ANOVA and Tukey *post hoc* test, the Lower fan exhibited the closest distance between patches, the minimum plant density, the largest patch sizes, and the lowest number of patches compared with other positions (Fig. 5a, b). Mean plant distance and mean vegetation density had a decreasing trend along slope from the Upper toward the Lower fan (Fig. 5a), and thus the lowest amount of vegetation density was occurred in the lower fan. Conversely, mean patch size increased down the debris fan with no significant differences between the Middle and Lower positions (Fig. 5b). The maximum average number of patches was observed on the Upper fan while the Lower and Middle positions had less, respectively (Fig. 5a).

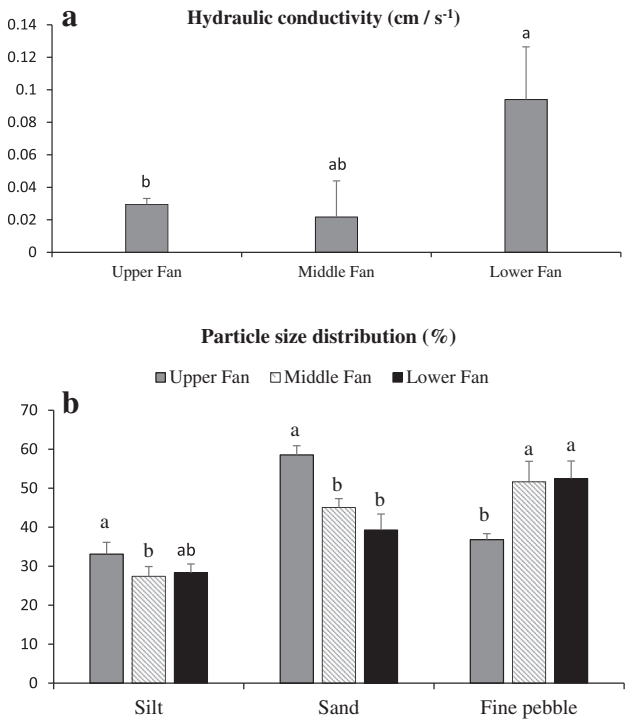

Fig. 4. Variations in infiltration rate (a) and particle size distribution (b) within different landform positions. Error bars and lowercase letters denote standard errors of means and statistically significant differences ($P < 0.05$) defined by Tukey *post hoc* test, for the different positions, respectively. Error bar represents standard error (*SE*) of soil properties differences within the positions.

Table 2
Results of one-way ANOVA and Tukey *post hoc* test of the comparison of vegetation properties at different positions within debris fan.

Position	Plant distance	Plant density	No. patches	Patch size
Upper Fan	530.6 ± 2.5^{a}	238.1 ± 7.0^{a}	99.2 ± 2.9^{a}	2373.1 ± 124.0^{b}
Middle Fan	490.0 ± 8.7^{b}	199.5 ± 8.6^{b}	53.0 ± 2.0^{b}	4006.6 ± 247.6^{a}
Lower Fan	409.8 ± 7.7^{c}	183.2 ± 3.8^{b}	36.2 ± 1.5^{c}	4087.2 ± 268.3^{a}

All values are mean ± standard error of the mean. Different lowercase letters show statistically significant differences ($P < 0.05$) among different positions of the study landform.

3.2. Biotic heterogeneities and the emergence of resilience thresholds along debris fan

The next research question examined whether fine scale significant heterogeneities in soil-dependent vegetation structures, within different landform positions, exhibit different levels of sustainability in response to the same rainfall gradient as environmental stress. To answer this question, after proving the statistically significant differences in the spatial patterns of vegetation properties in relation to soil heterogeneity in the study area, we ran the above reiterated model on some of the representative aerial images taken from the Upper, the Middle, and the

Table 1
Results of one-way ANOVA and Tukey *post hoc* test of soil particle size distribution (*PSD*) and hydraulic conductivity (K) within different debris fan positions.

Position	Clay (%) < 0.002 mm	Silt (%) 0.002–0.02 mm	Sand (%) 0.02–2 mm	Fine pebble (%) 2–12 mm	K (cm/s^{-1})	*df*
Upper Fan	32.3 ± 1.4	35.2 ± 3.0^{a}	58.5 ± 4.0^{a}	36.8 ± 1.5^{b}	0.024 ± 0.003^{b}	74
Middle Fan	27.8 ± 1.1	31.2 ± 2.5^{b}	45.0 ± 2.2^{b}	51.6 ± 5.2^{a}	0.045 ± 0.022^{ab}	74
Lower Fan	28.2 ± 0.9	28.2 ± 2.2^{ab}	39.3 ± 2.3^{b}	52.4 ± 4.4^{a}	0.098 ± 0.03^{a}	74

Note: All values are mean ± standard error of the mean. Different lowercase letters show statistically significant differences ($P < 0.05$) among different positions within the study landform.

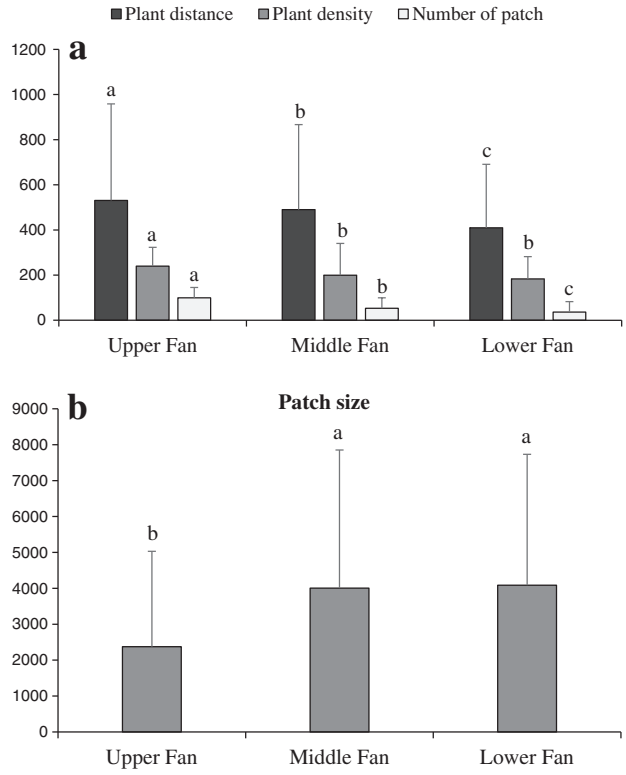

Fig. 5. Statistically significant differences of vegetation metrics including (a) mean plant distance, mean plant density, and the average number of patches, (b) mean patch size along different positions within the debris fan based on the results of Tukey *post hoc* test. Lowercase letters represent significant differences of means at 95% confidence level between the Upper, the Middle, and the Lower fan. Error bar represents standard deviation (*SD*) of vegetation metrics differences within the positions.

Lower fan plots. The results from the numerical simulations on the different positions within the debris fan presented that different positions of the fan responded differently over time to rainfall gradient, considering that aside from the input images which formed the initial conditions of the simulations, the initial values of all other parameters in the simulation were set the same.

The simulation results on the aerial images of the Upper fan showed three breakpoints in the behavior of this position over time to a gradual reduction of rainfall values (1.3, 0.8, 0.75 mm per day) (Fig. 6a). At a rainfall value 1.3 (breakpoint R1 in Fig. 6a), the position changed from a uniform vegetation state to patterned vegetation state. Note that these patterns are the onset sign of decreasing resilience of the system. Subcritical rainfall value of 0.8 mm/day (breakpoint R2 in Fig. 6a) led to the appearance of a state of periodic spot patterns. Finally, at critical rainfall value of 0.75 (threshold Rc in Fig. 6a) the transition from spot patterns state to desert state occurred.

The simulation results of the model on the Middle and Lower fan showed that the vegetation could survive under harsher conditions of aridity, in comparison with the Upper fan. Since the statistical differences between the positions of the Middle and Lower fan were not very strong, the simulations showed very similar results for both the positions. Fig. 6b shows four non-equilibrium thresholds in the response of the Middle fan position to different rainfall values (1.3, 0.75, 0.65, 0.63 mm per day). Breakpoint R1 corresponds to 1.3 mm/day rainfall and it is a point at which transition from uniform vegetation state to patterned state occurred. Breakpoint R2, which corresponds to 0.75 mm/day rainfall, is the point at which state of periodic spot patterns appeared. Breakpoint R3, which is associated with a subcritical rainfall of 0.65 mm/day, is the point at which the vegetation spots started to degrade until the desertification was complete. Breakpoint Rc, a critical rainfall of 0.63 mm/day, is the point at which the vegetation was lost and the land collapsed to desert state.

At the Lower fan position, four non-equilibrium thresholds can be seen in the behavior of this position to changing rainfall values (1.3, 0.65, 0.6, 0.58 mm per day) (Fig. 6c). Bifurcation R1, with rainfall value 1.3 mm/day, denotes the transition from uniform vegetation state to patterned state. Rainfall value 0.65 mm/day (breakpoint R2 in Fig. 6c) indicates the appearance of the spot patterned state. Breakpoint R3, with rainfall value 0.6 mm/day, indicates the subcritical phase at which periodic spot patterns state transforms to ring patterned state. Finally, at bifurcation Rc, which corresponds to a critical rainfall value of 0.58 mm/day, the Lower position of the fan demonstrated a critical transition to uniform barren state.

4. Discussion

4.1. Variations in spatial patterns of soil-vegetation properties within the debris fan: a cause for landscape heterogeneity

The analysis of the soil, infiltration and vegetation data showed how the local redistribution of debris flow-related sediments, with fine scale variations of surface soil properties, may exhibit heterogeneous eco-hydrological patterns. The results showed that the soil-dependent vegetation patterns may create invisible boundaries between different positions within the debris fan. They also showed that vegetation density and number of patches decreased as the coarse cover increased toward the Lower fan plots, while these metrics increased within the Upper fan plots with increasing the percentage of fine soil fractions. Further, although the plots at the Upper fan position had higher vegetation density, their soil exhibited the minimum amount of hydraulic conductivity compared with those of the plots located at the other positions of the fan. These heterogeneous eco-hydrological patterns can be explained by the subtle variations in surface soil texture, due to asymmetric redistribution of debris flow depositions. Since soil infiltration capacity is a major function of soil texture (Wood et al., 1987), showing consistency with the previous studies (Ravi et al., 2008), the reduced soil infiltration rate at the Upper fan can be explained by the increase in distribution of fine covers in comparison with the other positions. However our results differ from those of previous studies which claimed that the infiltration rate is higher under shrubs and decreases in interspaces (Bhark and Small, 2003; Bedford and Small, 2008; Ravi et al., 2008; Wu et al., 2016). Our results demonstrated that the Lower fan, despite having the lowest amount of vegetation density, exhibited the highest infiltration rate. Such eco-hydrological patterns indicate that moisture limitations may not be the reason for decreasing vegetation density. According to these results, the accumulation of coarse particles and lower capacity of these fractions for holding water and nutrients may have limited the vegetation growth at the Lower fan. Note that, the differences between the Middle and Lower fan were not as pronounced as those with the Upper fan position.

Despite recent efforts to explain the role of local redistribution in the activation of resource concentration, which seems to play a key role in the dynamic of arid landscapes (Wilcox et al., 2003; Rietkerk et al., 2004; Ludwig et al., 2005; Okin et al., 2006; Ravi et al., 2010), our understanding remains limited regarding the processes driving the redistribution of resources and how these processes affect the evolutionary trends of arid land landforms. Our results proved consistent with previous studies (Geertsema and Pojar, 2007; Geertsema and Highland, 2011), and show that debris flow can be a cause of landscape heterogeneity. One of the consequences of this disturbance is variation in site biotic-abiotic conditions at a given location (Geertsema and Pojar, 2007). Based on definition of Geertsema and Pojar (2007) site is a segment of landscape that is relatively uniform in terms of biotic-abiotic properties. The findings were shown that how heterogeneous redistribution of debris flows with making conditions drier or wetter (the result of hydraulic conductivity), or stonier or softer (the result of particle size distribution analysis) could stimulate the emergence of

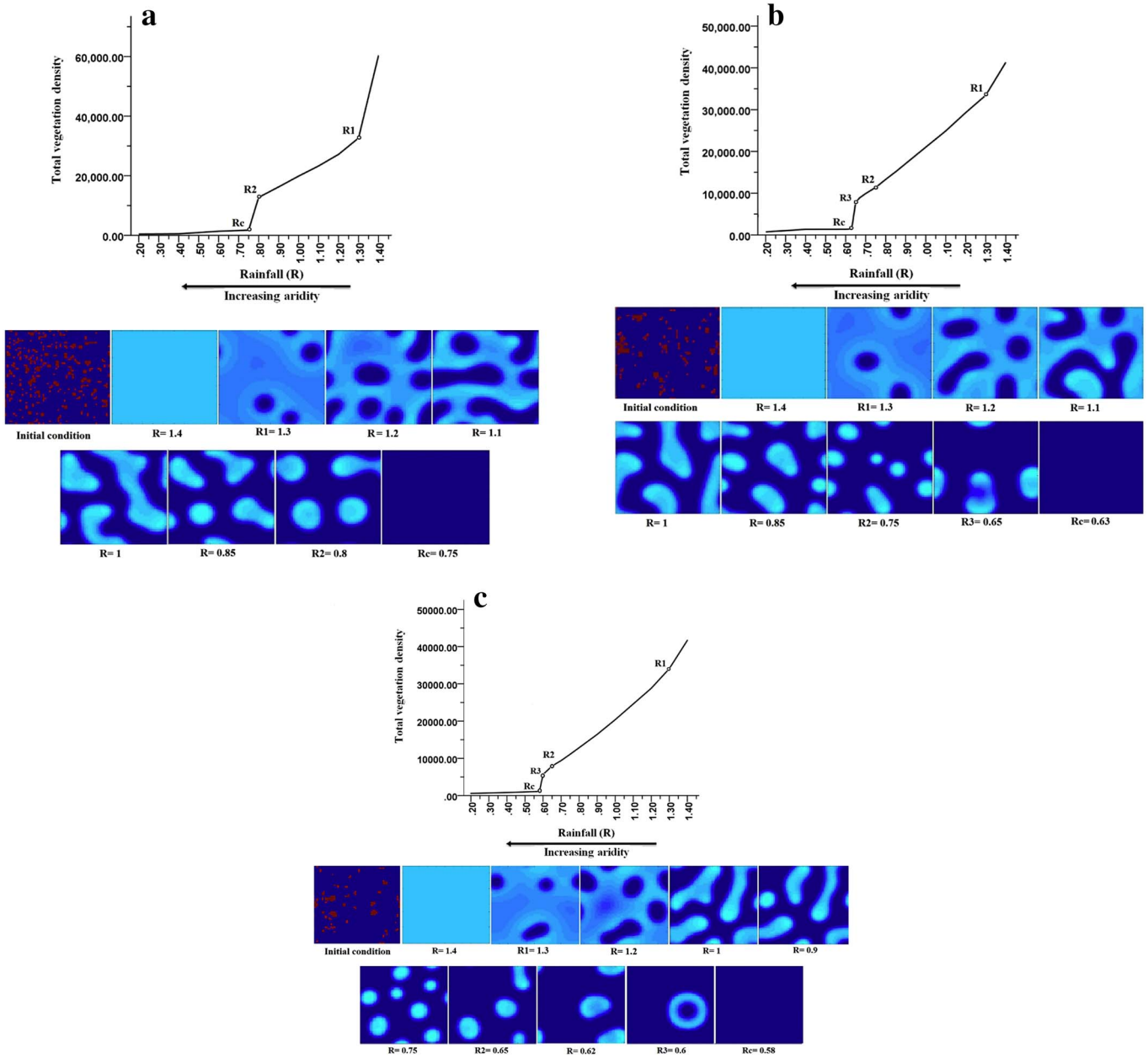

Fig. 6. A bifurcation diagrams (rainfall values at which the qualitative behavior of a system changes) of response trend of the Upper fan (a), Middle fan (b) and Lower fan (c) positions with increasing levels of aridity. This diagram indicates the total vegetation density *vs* precipitation. The images below the graphs are spatial snapshots of vegetation patterning as functions of decreasing rainfall up to desertification. Each image shows the last stationary state of the position at the end of 1000 time steps (years) for each discrete rainfall level. Open circles are the breakpoints R1, R2, R3, Rc showing sharp transitions between different vegetation states. Red spots at the first snapshots (initial conditions) are the current distribution of vegetation biomass within each position at commencement of modeling. Light blue and dark blue areas are vegetated and barren soils, respectively. The scale in all panels is the same. All parameter values are denoted in the method section. Rainfall value unit is millimeters per day. (For interpretation of the references to color in this figure legend, the reader is referred to the web version of this article.)

biotic-abiotic heterogeneities at given positions (Geertsema and Pojar, 2007). So that these heterogeneities could occur site conditions in the Upper, Middle, and Lower fan. The emergence of such localized variations (site conditions) within different landform positions resulted from changes in pattern of debris flow-induced soil properties promoted change of pattern of vegetation attributes within different sites (Geertsema et al., 2009).

Our findings demonstrated that fine-scale variability (site condition) in soil-dependent vegetation patterns within different landform positions depends strongly on the landform-dependent geomorphic processes (Bedford and Small, 2008) such as debris flows. This process may affect the local redistribution of sediment along the debris fan (Fig. 7). However, different landform positions respond differently to redistributed sediments. These various responses can appear as small scale spatial variations in the spatial patterns of soil and vegetation characteristics within different landform positions. These localized biotic-abiotic variations can exhibit multiple self-organization thresholds in the face of stressful conditions, in that each of these thresholds has different degrees of resistance which affect the dynamic trend of non-equilibrium landforms.

4.2. *Emergence of multiple resilience thresholds along debris fan: a consequence of landscape heterogeneity*

We tested whether different debris fan positions showing statistically significant differences in the distribution of soil-dependent biotic

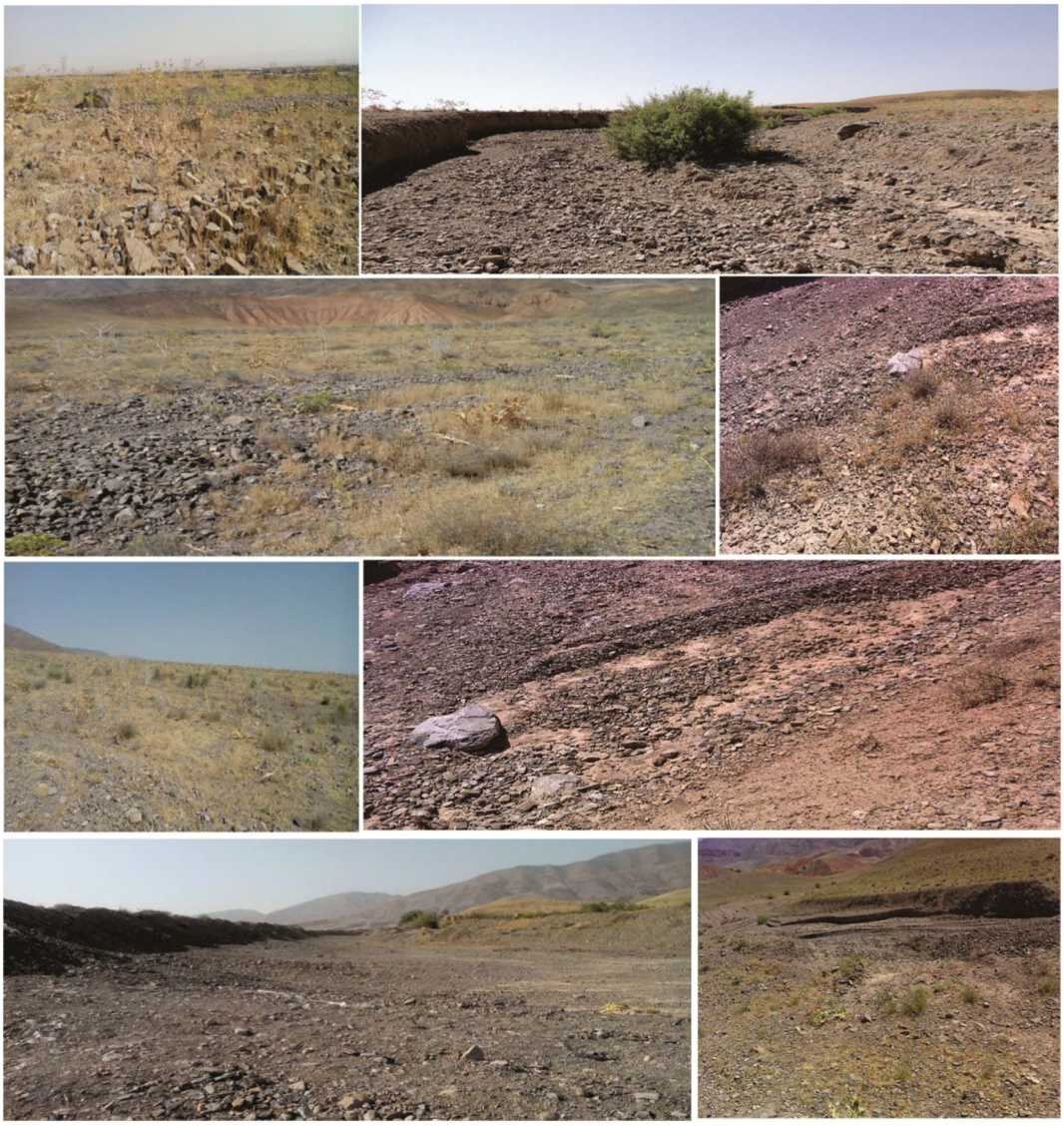

Fig. 7. Typical examples of the distribution of debris flow depositions along the study fan, at which accumulation of coarse covers results in limited vegetation growth.

structures, will respond similarly to the changes in rainfall over time. The simulation findings showed that despite the appearance of nearly similar signatures, which was mainly due to the nature of the model, the three positions respond differently to the increasing levels of aridity, in a way that desertification in different positions occurred from different ranges of rainfall values. We observed two basic differences in the dynamic of the Middle and Lower fan states compared with the Upper fan. Firstly, was the emergence of a larger bistability domain or area with transient stability that emerges between two different equilibrium levels such as dense vegetation and desert states in the same range of environmental conditions (such as rainfall value). The appearance of this domain is a sign of approaching desertification (Rietkerk et al., 2004; Kéfi et al., 2010) or transition from homogenously vegetated state to desert state. Secondly, there was the emergence of more varied sequences of spatial vegetation patterns: gaps, labyrinths, spots, and ring patterns before desertification.

For the Upper fan, the domain of bistability occurred under a smaller range of aridity levels, with no bistability in the transition from spot pattern state to desert state (Fig. 6a). Alternatively, bistability areas for the Middle and Lower fan appeared at higher aridity levels: breakpoints R1–R2 bordering uniform vegetation state and spot pattern state, and breakpoints R2–R3 between periodic spot patterns state and a uniform barren state (Fig. 6b, c).

For the Middle and Lower fan positions, the appearance of bifurcation R3 in the bistability range between periodic spot patterns state and uniform barren state saw two important manifestations. Firstly, a ring pattern formation and spot-like pattern indicated increasing the resilience level of these positions against increasing aridity. Secondly, the occurrence of these conditions saw the transition from spot pattern state to desert state as gradual and discontinuous. This implies that these positions could respond to harsher aridity conditions with a time delay. This was not the case for the Upper fan whose transition from spot pattern to desert state occurred as sudden and continuous. These differences resulted in increasing levels of self-organization and subsequent survival of vegetation under higher aridity levels in the Lower and Middle fan, than the Upper position (comparison of Fig. 6). The inconsistencies of the study positions in regard to the emergence of vegetation patterns and size of the bistability area under different aridity levels, suggest that there are considerable deviations in the behavior of different positions to the same environmental stresses. Taking into account the similarities of all model parameters, these deviations can be explained by variations in the current distribution of vegetation structures within the landforms. These variations, based on field observations, relate to different patterns of surface soil properties due to the heterogeneous redistribution of depositions of debris flows along the fan.

Formation of regular and irregular spatial vegetation patterns for forecasting desertification have been dealt with in some theoretical studies (von Hardenberg et al., 2001; Rietkerk et al., 2002; Rietkerk et al., 2004; Kéfi et al., 2010; Dakos et al., 2011; Meron, 2012; Kéfi et al., 2016). The findings of this study showed variations from those of some previous studies (Rietkerk et al., 2004; Kéfi et al., 2010), in that spot patterns may not always be the last occurring patterns before desertification and the transition from spot pattern state to desert state may be a gradual transition due to ring pattern formation according to the level of self-organization of the system (Meron, 2012). For the first time, a combined field and modeling approach was used to examine how landform-dependent processes with the occurrence of heterogeneities in soil-vegetation characteristics can demonstrate the heterogeneous self-organizations within different landform positions under the same environmental harshness. Our results indicate that the spatial heterogeneity of a landform state arising from the relationship between a geomorphic process (here debris flow) and biotic-abiotic variables can affect the resilience level of different landform positions in the face of external perturbations. Positions with greater heterogeneous distribution of vegetation (Middle and Lower fan) exhibit more self-organization of vegetation and a subsequent higher resilience under more stressful conditions. Alternatively, the homogenous positions in terms of the distribution of vegetation structures (Upper fan) could not survive under harsher aridity. In fact, increasing heterogeneity in the distribution of vegetation structures at the Lower position resulted in the establishment of self-organized patches that would not survive under higher aridity if homogeneously distributed, such as at the Upper position. Furthermore, the simultaneous appearance of these fine scale resilience thresholds, as a consequence of landscape heterogeneity with imposing asymmetric dynamics within different landform positions, can guarantee greater resilience of the whole landform to environmental harshness.

5. Conclusions

In this study, using a combination of field measurements and process-based modeling approach, we highlighted some of the causes and effects of landscape heterogeneity. From the results, it could be explained that landform-dependent processes such as debris flow, with the occurrence of fine scale heterogeneities in soil-dependent vegetation patterns, may exhibit multiple resilience thresholds and thereby encourage heterogeneous dynamics within different landform positions. The results showed that there were significant differences in the spatial patterns of soil and eco-hydrological properties between the Upper, Middle and Lower fan positions. So that, with increasing coarse soil fractions along the slope, infiltration rate increased and, subsequently the distribution of vegetation density was reduced. These variations in biotic and abiotic patterns can be explained by the asymmetric redistribution of debris flow depositions along landform. Further, the comparisons of the results of numerical simulations on the aerial images taken from different positions illustrated that the level of environmental harshness at which vegetation collapsed to a desert state was different among the positions. The Lower and Middle positions exhibited higher self-organization than the Upper fan, in the face of increasing aridity level. These findings may explain how geomorphic processes promote the emergence of biotic-abiotic heterogeneities and how such heterogeneities with the creation of multiple resilience thresholds can affect the dynamic trends of arid region landforms.

Acknowledgments

The authors are sincerely grateful to the editor, Prof. Markus Stoffel, and two anonymous reviewers for their consideration and constructive suggestions.

References

Bedford, D.R., Small, E.E., 2008. Spatial patterns of ecohydrologic properties on a hillslope-alluvial fan transect, central New Mexico. Catena 73, 34–48.
Bhark, E.W., Small, E.E., 2003. Association between plant canopies and the spatial patterns of infiltration in shrubland and grassland of the Chihuahuan Desert, New Mexico. Ecosystems 6, 0185–0196.
Bouyoucos, G.J., 1962. Hydrometer method improved for making particle size analyses of soils. Agron. J. 54, 464–465.
Breshears, D.D., Whicker, J.J., Zou, C.B., Field, J.P., Allen, C.D., 2009. A conceptual framework for dryland aeolian sediment transport along the grassland–forest continuum: effects of woody plant canopy cover and disturbance. Geomorphology 105, 28–38.
Bull, W.B., 1963. Alluvial-fan deposits in western Fresno County, California. J. Geol. 243–251.
Cartenì, F., Marasco, A., Bonanomi, G., Mazzoleni, S., Rietkerk, M., Giannino, F., 2012. Negative plant soil feedback explaining ring formation in clonal plants. J. Theor. Biol. 313, 153–161.
Couteron, P., Lejeune, O., 2001. Periodic spotted patterns in semi-arid vegetation explained by a propagation-inhibition model. J. Ecol. 89, 616–628.
Cruden, D.M., Varnes, D.J., 1996. Landslides: investigation and mitigation. Chapter 3: landslide types and processes. In: Transportation Research Board Special Report. 247.
Dakos, V., Kéfi, S., Rietkerk, M., Van Nes, E.H., Scheffer, M., 2011. Slowing down in spatially patterned ecosystems at the brink of collapse. Am. Nat. 177, E153–E166.
D'Odorico, P., Caylor, K., Okin, G.S., Scanlon, T.M., 2007. On soil moisture–vegetation feedbacks and their possible effects on the dynamics of dryland ecosystems. J. Geophys. Res. Biogeosci. 112, G04010.
Dorin Alexandru, P.O.P., CHIŢU, Z., 2013. Landslides and biodiversity conservation: the importance of an integrated approach. A case study: the subcarpathian part of the Doftana watershed (Prahova County, Romania). Revista de Geomorfologie 15, 57–68.
Geertsema, M., Highland, L.M., 2011. Landslides: human health effects. In: Nriagu, J.O. (Ed.), Encyclopedia of Environmental Health. vol. 3. Elsevier, Burlington, pp. 380–395.
Geertsema, M., Pojar, J.J., 2007. Influence of landslides on biophysical diversity—a perspective from British Columbia. Geomorphology 89 (1), 55–69.
Geertsema, M., Highland, L., Vaugeouis, L., 2009. Environmental impact of landslides. In: Landslides–Disaster Risk Reduction. Springer, Berlin Heidelberg, pp. 589–607.
Geertsema, M., Schwab, J.W., Jordan, P., Millard, T.H., Rollerson, T.P., 2010. Compendium of Forest Hydrology and Geomorphology in British Columbia, Chapter 8: Hillslope Processes. British Columbia Ministry of Forests and Rangepp. 213–273.
Graetz, R., Tongway, D.J., 1986. Influence of grazing management on vegetation, soil structure and nutrient distribution and the infiltration of applied rainfall in a semi-arid chenopod shrubland. Aust. J. Ecol. 11, 347–360.
von Hardenberg, J., Meron, E., Shachak, M., Zarmi, Y., 2001. Diversity of vegetation patterns and desertification. Phys. Rev. Lett. 87, 198101.
d'Herbès, J.-M., Valentin, C., Tongway, D.J., Leprun, J.-C., 2001. Banded vegetation patterns and related structures. In: Banded Vegetation Patterning in Arid and Semiarid Environments. Springer, pp. 1–19.
HilleRisLambers, R., Rietkerk, M., van den Bosch, F., Prins, H.H., de Kroon, H., 2001. Vegetation pattern formation in semi-arid grazing systems. Ecology 82, 50–61.
Hungr, O., Evans, S.G., Bovis, M.J., Hutchinson, J.N., 2001. A review of the classification of landslides of the flow type. Environ. Eng. Geosci. 7 (3), 221–238.
Kéfi, S., Rietkerk, M., Alados, C.L., Pueyo, Y., Papanastasis, V.P., ElAich, A., De Ruiter, P.C., 2007. Spatial vegetation patterns and imminent desertification in Mediterranean arid ecosystems. Nature 449, 213–217.
Kéfi, S., Eppinga, M.B., de Ruiter, P.C., Rietkerk, M., 2010. Bistability and regular spatial patterns in arid ecosystems. Theor. Ecol. 3, 257–269.
Kéfi, S., Holmgren, M., Scheffer, M., 2016. When can positive interactions cause alternative stable states in ecosystems? Funct. Ecol. 30, 88–97.
van de Koppel, J., Rietkerk, M., 2004. Spatial interactions and resilience in arid ecosystems. Am. Nat. 163, 113–121.
van de Koppel, J., Rietkerk, M., van Langevelde, F., Kumar, L., Klausmeier, C.A., Fryxell, J.M., Hearne, J.W., van Andel, J., de Ridder, N., Skidmore, A., 2002. Spatial heterogeneity and irreversible vegetation change in semiarid grazing systems. Am. Nat. 159, 209–218.
Ludwig, J.A., Wilcox, B.P., Breshears, D.D., Tongway, D.J., Imeson, A.C., 2005. Vegetation patches and runoff–erosion as interacting ecohydrological processes in semiarid landscapes. Ecology 86, 288–297.
Marston, R.A., 2010. Geomorphology and vegetation on hillslopes: interactions, dependencies, and feedback loops. Geomorphology 116, 206–217.
McDonald, A.K., Kinucan, R.J., Loomis, L.E., 2009. Ecohydrological interactions within banded vegetation in the northeastern Chihuahuan Desert, USA. Ecohydrology 2, 66–71.
Merino-Martín, L., Breshears, D.D., Moreno-de las Heras, M., Villegas, J.C., Pérez-Domingo, S., Espigares, T., Nicolau, J.M., 2012. Ecohydrological source-sink interrelationships between vegetation patches and soil hydrological properties along a disturbance gradient reveal a restoration threshold. Restor. Ecol. 20, 360–368.
Meron, E., 2012. Pattern-formation approach to modelling spatially extended ecosystems. Ecol. Model. 234, 70–82.
Moreno-de las Heras, M., Saco, P.M., Willgoose, G.R., Tongway, D.J., 2011. Assessing landscape structure and pattern fragmentation in semiarid ecosystems using patch-size distributions. Ecol. Appl. 21, 2793–2805.
Okin, G., Gillette, D., Herrick, J., 2006. Multi-scale controls on and consequences of aeolian processes in landscape change in arid and semi-arid environments. J. Arid

Environ. 65, 253–275.
Ravi, S., D'Odorico, P., Okin, G.S., 2007. Hydrologic and aeolian controls on vegetation patterns in arid landscapes. Geophys. Res. Lett. 34, L24S23.
Ravi, S., D'Odorico, P., Wang, L., Collins, S., 2008. Form and function of grass ring patterns in arid grasslands: the role of abiotic controls. Oecologia 158, 545–555.
Ravi, S., D'Odorico, P., Zobeck, T.M., Over, T.M., 2009. The effect of fire-induced soil hydrophobicity on wind erosion in a semiarid grassland: experimental observations and theoretical framework. Geomorphology 105, 80–86.
Ravi, S., Breshears, D.D., Huxman, T.E., D'Odorico, P., 2010. Land degradation in drylands: interactions among hydrologic–aeolian erosion and vegetation dynamics. Geomorphology 116, 236–245.
Rietkerk, M., Boerlijst, M.C., van Langevelde, F., HilleRisLambers, R., van de Koppel, J., Kumar, L., Prins, H.H., de Roos, A.M., 2002. Self-organization of vegetation in arid ecosystems. Am. Nat. 160, 524–530.
Rietkerk, M., Dekker, S.C., de Ruiter, P.C., van de Koppel, J., 2004. Self-organized patchiness and catastrophic shifts in ecosystems. Science 305, 1926–1929.
Saco, P., Willgoose, G., Hancock, G., 2007. Eco-geomorphology of banded vegetation patterns in arid and semi-arid regions. Hydrol. Earth Syst. Sci. 11, 1717–1730.
Scheffer, M., Carpenter, S., Foley, J.A., Folke, C., Walker, B., 2001. Catastrophic shifts in ecosystems. Nature 413, 591–596.
Scheffer, M., Bascompte, J., Brock, W.A., Brovkin, V., Carpenter, S.R., Dakos, V., Held, H., Van Nes, E.H., Rietkerk, M., Sugihara, G., 2009. Early-warning signals for critical transitions. Nature 461, 53–59.
Tongway, D.J., Ludwig, J.A., 2001. Theories on the origins, maintenance, dynamics, and functioning of banded landscapes. In: Banded Vegetation Patterning in Arid and Semiarid Environments. Springer, pp. 20–31.
Turnbull, L., Wainwright, J., Brazier, R.E., Bol, R., 2010. Biotic and abiotic changes in ecosystem structure over a shrub-encroachment gradient in the southwestern USA. Ecosystems 13, 1239–1255.
Turnbull, L., Wilcox, B.P., Belnap, J., Ravi, S., D'Odorico, P., Childers, D., Gwenzi, W., Okin, G., Wainwright, J., Caylor, K., 2012. Understanding the role of ecohydrological feedbacks in ecosystem state change in drylands. Ecohydrology 5, 174–183.
Wainwright, J., Parsons, A.J., Abrahams, A.D., 2000. Plot-scale studies of vegetation, overland flow and erosion interactions: case studies from Arizona and New Mexico. Hydrol. Process. 14, 2921–2943.
Walker, L.R., Shiels, A.B., 2012. Landslide Ecology. Cambridge University Press.
Wilcox, B.P., Breshears, D.D., Allen, C.D., 2003. Ecohydrology of a resource-conserving semiarid woodland: effects of scale and disturbance. Ecol. Monogr. 73, 223–239.
Wood, J.C., Wood, M.K., Tromble, J.M., 1987. Important factors influencing water infiltration and sediment production on arid lands in New Mexico. J. Arid Environ. 12, 111–118.
Wu, G.-L., Wang, D., Liu, Y., Hao, H.-M., Fang, N.-F., Shi, Z.-H., 2016. Mosaic-pattern vegetation formation and dynamics driven by the water–wind crisscross erosion. J. Hydrol. 538, 355–362.